Intrinsic relationship between electronic structures and phase transition of $SrBi_{2-x}Nd_xNb_2O_9$ ceramics from ultraviolet ellipsometry at elevated temperatures

Z. H. Duan (段志华), K. Jiang (姜凯), L. P. Xu (徐丽萍), Y. W. Li (李亚巍), Z. G. Hu (胡志高),[a] and J. H. Chu (褚君浩)

Key Laboratory of Polar Materials and Devices, Ministry of Education, Department of Electronic Engineering, East China Normal University, Shanghai 200241, China

(Received 1 December 2013; accepted 27 January 2014; published online 7 February 2013)

The ferroelectric orthorhombic to paraelectric tetragonal phase transition of $SrBi_{2-x}Nd_xNb_2O_9$ ($x = 0$, 0.05, 0.1, and 0.2) layer-structured ceramics has been investigated by temperature-dependent spectroscopic ellipsometry. Based on the analysis of dielectric functions from 0 to 500 °C with double Tauc-Lorentz dispersion model, the interband transitions located at ultraviolet region have shown an abrupt variation near the Curie temperature. The changes of dielectric functions are mainly due to the thermal-optical and/or photoelastic effect. Moreover, the characteristic alteration in interband transitions can be ascribed to distortion of NbO_6 octahedron and variation of hybridization between Bi 6*s* and O 2*p* states during the structure transformation.
 [http://dx.doi.org/10.1063/1.4864715]

I. INTRODUCTION

The Aurivillius family of Bismuth-layer-structured ferroelectrics (BLSFs) is promising candidate material for ferroelectric random-access memories, field-effect transistors and other optoelectronic devices.[1–3] Among them, $SrBi_2Nb_2O_9$ (SBN) has received considerable attention due to its low dielectric constants and excellent electro-optic properties.[2,4,5] The SBN structure consists of Bi_2O_2 layers and the perovskite-type $SrNb_2O_7$ units with double NbO_6 octahedra layers. Thus, physical properties can be tuned and improved through doping mechanisms into Bi sites or Sr(Nb)-sites in perovskite layers.[6,7] For example, Verma *et al*. reported that a phase transition from normal ferroelectric to paraelectric structure can be observed via relaxor-type ferroelectrics with addition of La^{3+} dopant.[8] Recently, lattice dynamics and dielectric behavior of Nd^{3+} doped SBN ($SrBi_{2-x}Nd_xNb_2O_9$, SBNN) ceramics have been studied by Raman scattering and infrared reflectance spectra.[4,7,9] However, the reported dielectric functions of SBNN ceramics have been only limited to infrared region and room temperature up to date. The dielectric functions in visible-ultraviolet photon energy range have not been concerned, which are practically important parameters for optoelectronic device design. Moreover, temperature evolution of the crystal structure and electronic band structure should be taken into consideration for high-temperature device applications. Especially, the dynamic behaviors of dielectric functions during ferroelectric-paraelectric (FE-PE) phase transition region which have been scarcely clarified, can lead to copious physical phenomena and the discovery of intrinsic mechanism about ferroelectric materials.

As a powerful spectral characterization technique, ellipsometry is based on the variation of the amplitude and phase of the incident polarized light after reflection from the samples. Spectroscopic ellipsometry (SE) is also recognized as a highly suitable method for determining the dielectric functions (ε) of materials over a wide spectral range.[10] Recently, SE has been widely applied to study the phase transitions, including magnetic spin reorientation transition,[11] metal-insulator transition,[12] and ferroelectric-paraelectric phase transition.[13,14] It is because phase transitions can be accompanied by changes of refractive index, energy band gap, and various other parameters that can be calculated from ellipsometric data.[15] Moreover, the dielectric function is directly related to the band structures and electronic transition by its imaginary part.

In this article, the Nd doping and temperature effects on the dielectric functions for SBNN ceramics from ultraviolet to near-infrared region have been studied. Intrinsic phase transition behaviors have been identified by inspecting the temperature evolution of interband transitions by SE technique.

II. EXPERIMENTAL DETAILS

The $SrBi_{2-x}Nd_xNb_2O_9$ ($x = 0$, 0.05, 0.1, and 0.2) ceramics were fabricated by a conventional solid-state reaction sintering. From the X-ray diffraction, the structure of SBNN ceramics belongs to the orthorhombic phase without impurity phases at room temperature.[4] All SBNN ceramic wafers were polished, rigorously cleaned in pure ethanol with an ultrasonic bath and rinsed several times by deionized water for the spectral measurements. Temperature-dependent SE experiments were carried out in the range of 1.24–6.4 eV at incident angle of 70° by a vertical variable-angle spectroscopic ellipsometer (J.A. Woollam Co., Inc.). The instrument was calibrated with the standard silicon wafer to record the window effect. The measurement was performed with the auto retarder (high accuracy) and the spectral resolution is set to 5 nm. The samples are mounted

[a]Author to whom correspondence should be addressed. Electronic mail: zghu@ee.ecnu.edu.cn. Tel.: +86-21-54345150. Fax: +86-21-54345119.

into an Instec cell with liquid nitrogen cooling accessory and frame water pump cooling for variable-temperature measurements. The temperature range is varied from 0 to 500 °C with the set-point stability of better than 1 °C. Ellipsometric data were directly analyzed with the software package WVASE32 which allows window corrections to be included as a part of the model used for analysis.

III. RESULTS AND DISCUSSION

Figures 1(a)–1(d) present the complex dielectric functions $[\tilde{\varepsilon}(\omega) = \varepsilon_1 + i\varepsilon_2]$ for SBNN ceramics determined by SE analysis. These data were calculated directly without correction for any coating or overlayer effect due to the severely double-polishing process. In general, the imaginary part ε_2 of $\tilde{\varepsilon}(\omega)$ has a slightly increase with increasing photon energy below 3 eV. As the photon energy further increases, the ε_2 sharply increases due to a strong optical absorption and then decreases to the present measurement limitation. Meanwhile, the parameter ε_1 increases with the photon energy and approaches the maximum, then decreases with further increasing photon frequency due to the known Van Hove singularities. Compared to pure SBN ceramic, the rising edge of Nd-doped SBN shifts towards a higher energy side. With increasing Nd composition, the rising edge shows a blue shift pattern except for the SBNN ($x = 0.2$). For example, the values of ε_2 at 4 eV (300 °C) are estimated to be 3.77, 3.17, 2.92, and 3.09, respectively. It means that Nd dopant induces the increment of onset energy for optical absorption, indicating the Nd influence on the band structures of SBN ceramics. As can be seen in Figure 1, when the temperature increases, the peak of ε_1 flattens and the value of ε_1 increases. Below 3 eV, the value of ε_1 increases with increasing the temperature, while the value of ε_2 decreases. As an example, the temperature evolution of dielectric functions for SBNN ceramics at 2 eV is shown in Figure 2. For the SBNN ceramics ($x = 0$, 0.05, 0.1), the value of ε_1 rises linearly (from 0 °C to 435, 390, and 350 °C, respectively) and saturates at the higher temperatures. For SBNN ($x = 0.2$)

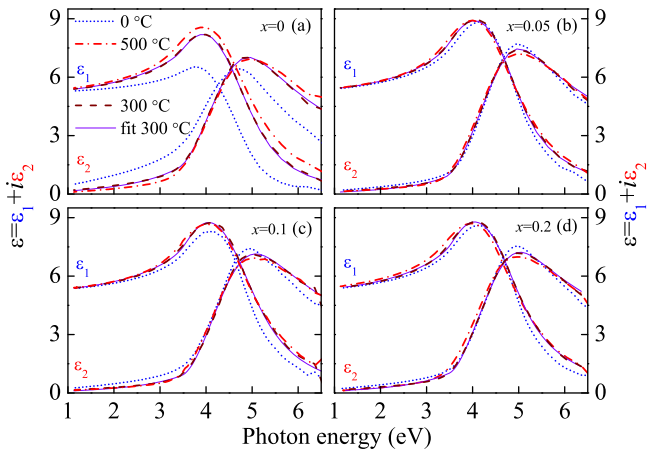

FIG. 1. Complex dielectric functions derived from SE measurements at several temperatures for $SrBi_{2-x}Nd_xNb_2O_9$ ceramics with different Nd compositions: (a) $x = 0$, (b) $x = 0.05$, (c) $x = 0.1$, and (d) $x = 0.2$, respectively. Note that the solid lines indicate the fitted spectra with Tauc-Lorentz model at 300 °C.

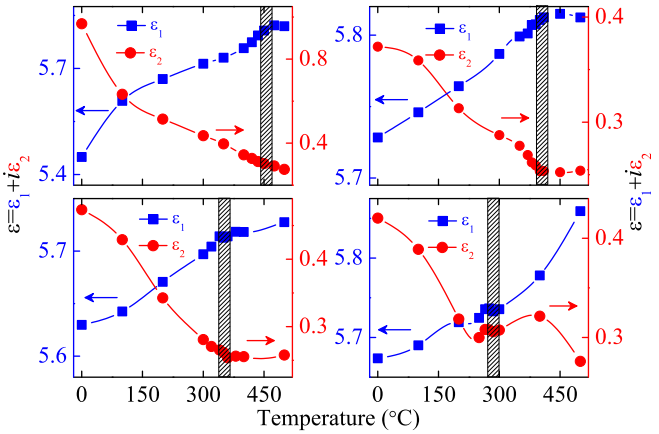

FIG. 2. The real (ε_1) and imaginary (ε_2) parts of the dielectric functions at 2 eV as a function of temperature for the SBNN ceramics [(a) $x = 0$, (b) $x = 0.05$, (c) $x = 0.1$, and (d) $x = 0.2$]. The striations indicate the phase transition regions from paraelectric to ferroelectric structure.

ceramic, however, the ε_1 monotonically increases on heating and rises faster in the high temperature region. The parameter ε_2, which obeys the Kramers-Kronig relations with the real part ε_1, presents an opposite trend. The dielectric function is closely associated with electronic band structures, which depends on the crystal structure. Thus, the dielectric function $\tilde{\varepsilon}$ is expected to change when the structural transition occurs in the ceramics. In Figure 2, the specific turning sections are marked with striations, which can demonstrate the structural transformation (Curie temperature, T_c) from ferroelectric to paraelectric phase.

It was assumed that the changes of dielectric permittivity with the temperature can be written as: $\Delta B_{ij} = (\mu_{ij} + p_{ijkl}\alpha_{kl})\Delta T$,[16] where μ_{ij} is the thermal-optical effect (TOE) tensor controlled by the electron-phonon interaction, α_{kl} is the thermal expansion coefficient and p_{ijkl} is photoelastic coefficient. The variations of refractive index $\delta(n) = -X\delta B_{ij}$, here, X depends on the crystal symmetry. With the formulas $\varepsilon_1 = n^2 - \kappa^2$ and $\varepsilon_2 = 2n\kappa$, it can be further concluded that the expressions $d\varepsilon_1/dT = 2n(dn/dT) - 2\kappa(d\kappa/dT)$; $d\varepsilon_2/dT = 2\kappa(dn/dT) + 2n(d\kappa/dT)$. Here, n and κ is refractive index and extinction coefficient, respectively. The value of κ is small enough (<0.1) at 2 eV and has a slightly decrease with the temperature. Therefore, the evolution of ε_1 is mainly related to the TOE, thermal expansion and effect caused by the absorption.[15,16] Generally, the photoelastic mechanical deformation leads to the reduction of ε_1 with increasing the temperature. Below the T_c, the SBNN ceramics belong to the ferroelectric phase with orthorhombic structure (space group $A2_1am$). In this region, the real part ε_1 becomes larger and imaginary part ε_2 reduces with increasing the temperature from Figure 2. The positive $d\varepsilon_1/dT$ and negative $d\varepsilon_2/dT$ values indicate that the electron-phonon interaction is more prominent than the photoelastic effect. When the temperature is beyond T_c, the structure transforms into a tetragonal paraelectric phase with space group $I4/mmm$. The real part ε_1 for SBNN ($x = 0$, 0.05, and 0.1) almost keeps constancy or sharply increases ($x = 0.2$), which can be due to the change of structure symmetry. To completely study the phase transition, the interband transitions in

TABLE I. The transition energy (E_{p1}, E_{p2}) parameters of Tauc-Lorentz model for $SrBi_{2-x}Nd_xNb_2O_9$ ceramics are extracted from the best fitting of dielectric functions at 0, 300, and 500 °C, respectively. Note that all parameters are in unit of photon energy (eV).

Samples	$x=0$			$x=0.05$			$x=0.1$			$x=0.2$		
Temp. (°C)	0	300	500	0	300	500	0	300	500	0	300	500
E_{p1}	3.70	3.92	3.79	4.04	4.01	3.96	3.95	4.01	3.92	3.99	4.00	3.92
	(0.19)	(0.26)	(0.10)	(0.29)	(0.21)	(0.19)	(0.57)	(0.23)	(0.19)	(0.33)	(0.22)	(0.17)
E_{p2}	4.78	4.83	4.79	4.94	4.91	4.89	4.90	4.94	4.89	4.93	4.91	4.86
	(0.14)	(0.04)	(0.02)	(0.04)	(0.03)	(0.03)	(0.04)	(0.06)	(0.03)	(0.03)	(0.02)	(0.02)

the absorption region are also discussed as follows. It should be noted that the T_c decreases with increasing Nd composition, which is consistent with those derived by Raman scattering and dielectric permittivity measurements.[7,9]

In order to extract the critical parameters of the band-band transitions, the dielectric response of the SBNN ceramics are analyzed via fitting with double Tauc-Lorentz (DTL) oscillators model. The formula can be written:[17,18]

$$\varepsilon_1(E) = \varepsilon_\infty + \frac{2}{\pi} P \int_0^\infty \frac{\xi \varepsilon_2(E)}{\xi^2 - E^2} d\xi, \quad \varepsilon_2(E) = \sum_{i=1}^{2} \frac{A_i E_{pi} \Gamma_i (E - E_{ti})^2}{(E^2 - E_{pi}^2)^2 + \Gamma_i^2 E^2} \frac{1}{E},$$

where ε_∞ is the high-frequency dielectric constant, P is the Cauchy principal part of the integral, and E is the incident photon energy. Also, A_i, E_{pi}, Γ_i, and E_{ti} are the amplitude, peak position energy, broadening term, and Tauc gap energy of the ith oscillator, respectively. Fig. 1 displays the experimental and fitted dielectric functions at 300 °C with the dotted and solid lines, respectively. The values of E_{p1} and E_{p2} at several temperatures are listed in Table I. According to the first-principles calculations on the electronic structures of SBN, it was found that SBN is a typical displacive-type FE transition-metal oxide and the valence bands (VB) are primarily from O 2p states and mixed with Nb 4d, Bi 6s and Bi 6p states.[2,5,19] The conduction band (CB) edge is determined mainly by Nb 4d and Bi 6p states. The O 2p states also make contributions to high energy side of CB.[2] Due to the complex nature of electronic structures, multiple transitions may happen at the same energy peak positions. Therefore, the inter-band transitions cannot be strictly assigned. Nevertheless, they can be attributed to the transitions from the O 2p states to the Nb 4d and/or the hybridization states tentatively. As for the SBN ceramics, the perovskite $SrNb_2O_7$ units is under compressive stress while Bi_2O_2 layer is under tensile stress.[7] The substitution of Bi^{3+} by Nd^{3+} can lead to the modulation of stress and rearrangement of the structural framework, particularly into the $[(Bi, Nd)_2O_2]$ layers, which will affect the electronic band structures.

The peak position energies and broadening derived from the DTL model as a function of temperature are shown in Figure 3. The linear fitting of transition energies can be performed in two different temperature regions and the critical point temperature is labeled by the vertical lines. Taking SBNN ($x=0.2$) as an example, the slope of linear temperature dependence for E_{p1} and E_{p2} shows the distinct variation between the two regions. The slope of the fitted line for E_{p1} in the high temperature region is -2.37×10^{-4} eV/°C, while the slope is estimated to be 1.28×10^{-4} eV/°C in the low temperature part. As a whole, the broadening Γ_1 becomes larger with increasing the temperature. However, the parameter Γ_2 slightly decreases first and then increases beyond the critical temperature. The critical temperature of E_{pi} ($i=1$, 2) and Γ_i ($i=1$, 2) confirms the studies of T_c (FE-PE transition) at which the structure transformation takes place. It was reported that the transition from a paraelectric tetragonal to ferroelectric orthorhombic phase can induce large distortions in the crystal structure for pure SBN, especially for the electron-density distributions in the bonding of NbO_6 octahedron.[2] Compared with the PE phase, the orbital hybridization between Nb 4d and O 2p is enhanced, which leads to anisotropic electron-density distribution.[2,19] The physical behavior is similar to that found in $SrBi_2Ta_2O_9$ (SBT) and $PbTiO_3$.[20,21] Furthermore, four symmetry-inequivalent Bi-O bond lengths between Bi atom (Bi_{22} layers) and apical O

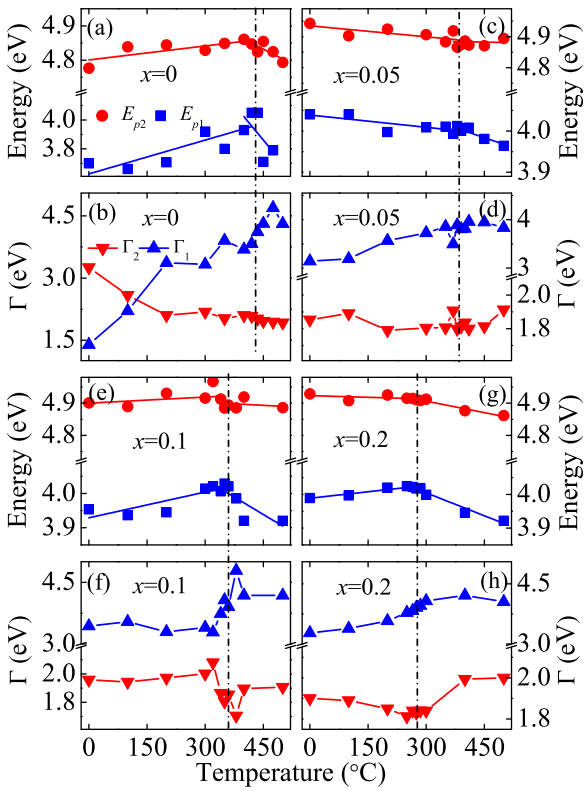

FIG. 3. Temperature dependence of peak positions (E_{p1} and E_{p2}) and broadening terms (Γ_1 and Γ_2) of two oscillators for the SBNN ceramics. The linear fitting was performed on the variation of E_{p1} and E_{p2} with the temperature, as shown by solid lines. The solid lines for the parameters Γ_1 and Γ_2 are only used to guide the eyes. Note that the dashed lines suggest the PE-FE transition temperature.

atom (perovskite block) becomes one when the structure changes from polar orthorhombic to centrosymmetric tetragonal,[22] which can remarkably influence the density distribution of Bi and O atoms. There also is weak hybridization between Bi and O in the valence band and Bi 6*s* contribution can be almost neglected at the top of VB in the paraelectric phase. However, the Bi 6*s* states shift to the Fermi surface and a significant mixing between Bi 6*s* and O 2*p* appears at the top of VB in the ferroelectric phase.[19] It should be noted that the Nd 4*d* states shifts towards a higher energy side in the ferroelectric phase. These phenomena indicate that the conduction band and valence band edges change obviously during the PE-FE transition, which reveals that the structure variation has a remarkable influence on the electronic structures. It should be emphasized that the transition temperature T_c decreases with increasing Nd composition, as shown in Figure 3. Since the lone pair electrons tend to occupy more space than bonding pairs, the Nd (has no lone-pair electrons) doping can induce the reduction of tilting degree and/or distortion extent of NbO_6 octahedron,[7] leading to the decrease of Curie temperature. Therefore, the assignments of FE-PE phase transition are not only based on the temperature evolution of dielectric functions, but also derived from the interband transitions with the aid of the DTL dispersion model. These results indicate that SE could be an acceptable method to clarify the phase transition of ferroelectric materials.

IV. CONCLUSIONS

In summary, the temperature dependence of interband transition and electronic structures for $SrBi_{2-x}Nd_xNb_2O_9$ ceramics have been investigated by spectroscopic ellipsometry. The PE-FE structure phase transition can be well recognized through the variation of dielectric functions and transition energies, which is closely related to the hybridization between Bi and O and the distortion of NbO_6 octahedron. The present study confirms that spectroscopic ellipsometry is an effective means to study the phase/structure transition.

ACKNOWLEDGMENTS

This work was financially supported by Major State Basic Research Development Program of China (Grant Nos. 2011CB922200 and 2013CB922300), Natural Science Foundation of China (Grant Nos. 11374097, 61376129, 61106122, and 11074076), Projects of Science and Technology Commission of Shanghai Municipality (Grant Nos. 13JC1402100 and 13JC1404200), and the Program for Professor of Special Appointment (Eastern Scholar) at Shanghai Institutions of Higher Learning.

[1]C. A-Paz de Araujo, J. D. Cuchiaro, L. D. McMillan, M. C. Scott, and J. F. Scott, Nature (London) **374**, 627 (1994).
[2]Y. Shimakawa, H. Imai, H. Kimura, S. Kimura, Y. Kubo, E. Nishibori, M. Takata, M. Sakata, K. Kato, and Z. Hiroi, Phys. Rev. B **66**, 144110 (2002).
[3]A. Srinivas, T. Sritharan, and F. Y. C. Boey, J. Appl. Phys. **98**, 036104 (2005).
[4]M. Zhu, L. Sun, W. W. Li, W. L. Yu, Y. W. Li, Z. G. Hu, and J. H. Chu, Mater. Res. Bull. **45**, 1654 (2010).
[5]K. Miura, Appl. Phys. Lett. **80**, 2967 (2002).
[6]P. Millán, A. Ramirez, and A. Castro, J. Mater. Sci. Lett. **14**, 1657 (1995).
[7]L. Sun, C. D. Feng, L. D. Chen, and S. M. Huang, J. Appl. Phys. **101**, 084102 (2007).
[8]M. Verma, K. Sreenivas, and V. Gupta, J. Appl. Phys. **105**, 024511 (2009).
[9]K. Jiang, W. W. Li, X. G. Chen, Z. N. Zhan, L. Sun, Z. G. Hu, and J. H. Chu, J. Raman Spectrosc. **43**, 583 (2012).
[10]S. G. Choi, H. Y. Zhao, C. Persson, C. L. Perkins, A. L. Donohue, B. To, A. G. Norman, J. Li, and I. L. Repins, J. Appl. Phys. **111**, 033506 (2012).
[11]B. Berini, A. Fouchet, E. Popova, J. Scola, Y. Dumont, N. Franco, R. M. C. da Silva, and N. Keller, J. Appl. Phys. **111**, 053923 (2012).
[12]M. Nazari, Y. Zhao, V. V. Kuryatkov, Z. Y. Fan, A. A. Bernussi, and M. Holtz, Phys. Rev. B **87**, 035142 (2013).
[13]M. Tyunina, A. Dejneka, D. Chvostova, J. Levoska, M. Plekh, and L. Jastrabik, Phys. Rev. B **86**, 224105 (2012).
[14]Z. H. Duan, Z. G. Hu, K. Jiang, G. S. Wang, X. L. Dong, and J. H. Chu, Appl. Phys. Lett. **102**, 151908 (2013).
[15]A. Dejneka, I. Aulika, V. Trepakov, J. Krepelka, L. Jastrabik, Z. Hubicka, and A. Lynnyk, Opt. Express **17**, 14322 (2009).
[16]V. Trepakov, A. Dejneka, P. Markovin, A. Lynnyk, and L. Jastrabik, New J. Phys. **11**, 083024 (2009).
[17]J. G. E. Jellison and F. A. Modine, Appl. Phys. Lett. **69**, 371 (1996); **69**, 2137 (1996).
[18]X. Chen, K. Jiang, Z. G. Hu, X. F. Chen, G. S. Wang, X. L. Dong, and J. H. Chu, Appl. Phys. Lett. **101**, 011914 (2012).
[19]H. B. Shu, L. Z. Sun, X. L. Zhong, J. B. Wang, and Y. C. Zhou, J. Phys. Chem. Solids **70**, 707 (2009).
[20]M. G. Stachiotti, C. O. Rodriguez, C. Ambrosch-Draxl, and N. E. Christensen, Phys. Rev. B **61**, 14434 (2000).
[21]J. Zhang, Z. Yin, and M. S. Zhang, Appl. Phys. Lett. **81**, 4778 (2002).
[22]A. Snedden, C. H. Hervovhes, and P. Lightfoot, Phys. Rev. B **67**, 092102 (2003).